

# Cosmic Muon Detection: Lifetime and g-factor measurements

Daniel Forero, Claire Blaga, Marco Hartmann

Supervisor: Tara Nanut

Professor: Olivier Schneider

January 9, 2019

## Abstract

The aim of this research project is to experimentally determine the average lifetime of cosmic muons by stopping them in a copper plate and measuring the time taken for them to decay. With the use of a simple experimental apparatus consisting of a copper plate, scintillators, photomultiplier tubes (PMTs), nuclear instrumentation modules (NIM) and an appropriate trigger scheme, an average muon decay lifetime of  $\tau_{\mu,d} = 2.317 \pm 0.082 \mu\text{s}$  was measured. This experimental result has a deviation of 5% from the value found in literature  $\tau_d = 2.196981 \pm 0.000002 \mu\text{s}$ . Negative muons, subject to nucleon capture, were found to have a capture lifetime in copper of  $\tau_{\mu,c} = 0.270 \pm 0.056 \mu\text{s}$ . In this case, there is a 69% deviation from the tabulated value  $\tau_c = 0.16 \mu\text{s}$ . In both cases, the tabulated values are not within the experimental uncertainties but further analyses should be undertaken, taking into account the possible systematic errors.

Furthermore, by generating a magnetic field with Helmholtz coils, the g-factor of cosmic muons was measured and compared to the theoretical value. In this second part of the experiment, a value of  $g = 1.909 \pm 0.096$  was obtained, indeed covering the value of  $g = 2$  predicted by Dirac theory in its uncertainty margin. However, the large experimental error prevents finding the associated anomalous moment. To find this, one could increase the accuracy by taking more data, varying the magnetic field and using a more accurate apparatus.

## Contents

<b>1</b>	<b>Introduction</b>	<b>3</b>
<b>2</b>	<b>Background theory</b>	<b>3</b>
2.1	Muon lifetime . . . . .	3
2.2	Lifetime of the positive and negative muons . . . . .	4
2.3	Muons in magnetic field . . . . .	4
<b>3</b>	<b>Apparatus</b>	<b>5</b>
3.1	Particle detection . . . . .	5
3.2	Magnetic field . . . . .	6
<b>4</b>	<b>Experimental setup</b>	<b>6</b>
4.1	Trigger scheme . . . . .	7
4.2	PMT voltage calibration . . . . .	7
4.3	Discriminator threshold calibration . . . . .	8
<b>5</b>	<b>Results</b>	<b>10</b>
5.1	Muon lifetime . . . . .	10
5.2	$g$ -factor measurement . . . . .	13
<b>6</b>	<b>Discussion</b>	<b>14</b>
<b>7</b>	<b>Conclusion</b>	<b>15</b>

## 1 Introduction

Cosmic muons result from the interaction of cosmic rays containing high energy particles with the Earth's upper atmosphere. This interaction produces a hadronic shower containing charged  $\pi^\pm$  mesons which can decay into high energy muons:

$$\pi^+ \rightarrow \mu^+ \nu_\mu \qquad \pi^- \rightarrow \mu^- \bar{\nu}_\mu \quad (1)$$

These cosmic muons will then decay into electrons or positrons and neutrinos:

$$\mu^+ \rightarrow e^+ \nu_e \bar{\nu}_\mu \qquad \mu^- \rightarrow e^- \bar{\nu}_e \nu_\mu \quad (2)$$

Muons have an average lifetime of  $\tau = 2.196981 \pm 0.000002 \mu\text{s}$  [1]. Since they travel at almost the speed of light, it should take them approximately  $50\mu\text{s}$  to reach the Earth's surface from the position of their formation 15km above sea level. Thus, no cosmic muons should be detected on Earth. However, this is not the case due to time dilation since muons are relativistic particles. This experiment aims to reproduce the findings of the average muon lifetime by stopping the cosmic particles in a copper plate and measuring the time taken for them to decay. The g-factor relating the muon's magnetic moment to its spin will also be found by applying a magnetic field to the experiment.

## 2 Background theory

### 2.1 Muon lifetime

Since the decay of a particle follows a Poisson distribution, it is therefore a process with constant probability as shown by equation (3):

$$dP = \lambda dt \quad (3)$$

where  $dP$  is the differential probability that a decay will occur during an infinitesimal time  $dt$ .  $\lambda$  is therefore the probability per unit time for a decay to occur, called the decay constant. The number of decays during a time  $dt$  is thus given by equation (4).

$$dN = -\lambda N dt \quad (4)$$

By solving this differential equation, the distribution of the decays can be obtained as shown by equation (5).

$$N(t) = N_0 e^{-\lambda t} \quad (5)$$

The average time before the decay of a particle occurs is calculated as shown by equation (6).

$$\langle t \rangle = \frac{\int_0^\infty t N(t) dt}{\int_0^\infty N(t) dt} = \frac{1}{\lambda} = \tau \quad (6)$$

$\tau$  is therefore the average lifetime of the particle. For muons, this value is  $\tau_\mu = 2.196981 \pm 0.000002 \mu\text{s}$ . [1]

## 2.2 Lifetime of the positive and negative muons

Positive and negative muons behave differently from each other in matter. This is, of course, relevant to the experiment since as described in section 3, the measurement procedure used involves stopping the muons in a copper plate.

Positive muons decay within the material as they would in a vacuum. However, negative muons have a high chance of being captured by the nuclei of the atoms of the medium surrounding them due to their similar properties to electrons. The processes that describe the decay of muons in matter are therefore

$$\mu^+ \longrightarrow e^+ \nu_e \bar{\nu}_\mu, \quad (7)$$

$$\mu^- \longrightarrow e^- \bar{\nu}_e \nu_\mu, \quad (8)$$

$$\mu^- p \longrightarrow n \nu_\mu. \quad (9)$$

For negative muons, the total decay constant is therefore  $\lambda^- = \lambda_d + \lambda_c$ , where  $\lambda_d$  is the decay constant for normal muon decay and  $\lambda_c$  is the decay constant for nucleon capture. The total lifetime of negative muons which will be measured is therefore

$$\frac{1}{\tau^-} = \frac{1}{\tau_d} + \frac{1}{\tau_c} \quad (10)$$

with the lifetimes  $\tau_d$  and  $\tau_c$  of the decay and capture processes. The decay lifetime is  $\tau_d \approx 2.2\mu\text{s}$  and the capture one depends on the material. More precisely, it depends on its atomic number  $Z$  [2] as:

$$\lambda_c(Z) = \lambda_1 Z^4 \quad (11)$$

where  $\lambda_1$  is the decay rate of negative muons in hydrogen.

This means that in copper,  $\tau_c = \frac{1}{\lambda_c} = 0.16\mu\text{s}$  [3]. Therefore

$$\tau^- = \left( \frac{1}{\tau_d} + \frac{1}{\tau_c} \right)^{-1} \approx \left( \frac{1}{\tau_c} \right)^{-1} = \tau_c \quad (12)$$

Since positive muons are not captured by the medium's nuclei, their lifetime is the usual  $\tau^+ = \tau_d = 2.2\mu\text{s}$ . The experiment will therefore aim to measure the lifetime of the positive muons as they are not affected by the medium and thus, reflecting the true average lifetime of muons.

## 2.3 Muons in magnetic field

Neutrinos are particles with the property that they always have a left handed helicity. This means that the direction of their spin and momentum are opposite. In the rest frame of the pion, which decays into a muon and a neutrino, it can be deduced from the fact that pions have no spin that the muon must have its spin in the opposite direction to that of the neutrino in order to have spin conservation. Thus, neutrinos being left handed, the muons will be right handed. From the spin  $S$  of the muons, a spin magnetic moment (13) arises:

$$\vec{\mu} = g\mu_{Bohr}\vec{S} = g\frac{q\hbar}{2m_\mu}\vec{S} \quad (13)$$

where  $\mu_{Bohr}$  is the Bohr magneton with  $q$  the electric charge of the muon,  $\hbar$  the reduced Planck constant and  $m_\mu$  the mass of the muon. Furthermore,  $g$  is a dimensionless number called the g-factor, with Dirac theory predicting  $g = 2$  for muons. However, quantum electrodynamics calculations considering higher order corrections predict a deviation from this value which is characterized by the anomalous magnetic moment (14):

$$a = \frac{g - 2}{2} \quad (14)$$

If the spin of the muon has a perpendicular component to the applied magnetic field  $B$ , the magnetic moment will cause the muon to precess around the direction of the magnetic field at the Larmor frequency (15):

$$\omega_L = g \frac{qB}{2m_\mu} \quad (15)$$

When the muon decays (equations 7 and 8), the electron or positron will be emitted according to the spatial distribution [4]:

$$N(\theta) \propto 1 + A \cos(\theta) \quad (16)$$

where  $\theta$  is the angle between the emitted electron (positron) and the spin of the muon.  $A$  is the asymmetry parameter which depends on the energy of the emitted electron (positron);  $A = 1$  when the energy is maximal,  $A = 1/3$  when averaging over all decay energies. Therefore, the time dependent number of counts will be given by:

$$N(t) = N_0 e^{-t/\tau} (1 + P A \cos(\omega_L t + \phi)) \quad (17)$$

where  $P$  is the polarization of the cosmic muon produced by the asymmetry of the decay and  $\phi$  is the angle between the detection direction and the spin of the muon.

### 3 Apparatus

#### 3.1 Particle detection

The detection of the passing of cosmic muons and their decay products is done through the use of scintillators. These are luminescent materials; the valence electrons of the atoms are excited when a charged particle or a photon passes through. They then undergo radiative relaxation almost instantaneously, thus emitting a photon in a fluorescent process. The emitted photon is conducted through the scintillator by a light guide to the photomultiplier tube (PMT). PMTs operate based on the photoelectric effect and secondary electron emission. When the photon emitted in the scintillator reaches the PMT, it hits a photocathode, emitting electrons by photoelectric effect which are directed onto the first dynode by a focusing electrode as shown by Figure 1. The collision of the electrons onto the metallic surface of the dynode induces the emission of secondary electrons. These are then attracted to the next dynode by a constant potential difference between consecutive dynodes, producing an avalanche of electrons by secondary emission. At the final stage, the electrons are collected at an anode to give an electric signal. The latter depends on the voltage between the photocathode and the anode. The signals detected are then passed through nuclear instrumentation modules (NIM) to select which ones will start and stop the clock measuring the time taken for the muons to decay. The modules used are the following:

## 4 EXPERIMENTAL SETUP

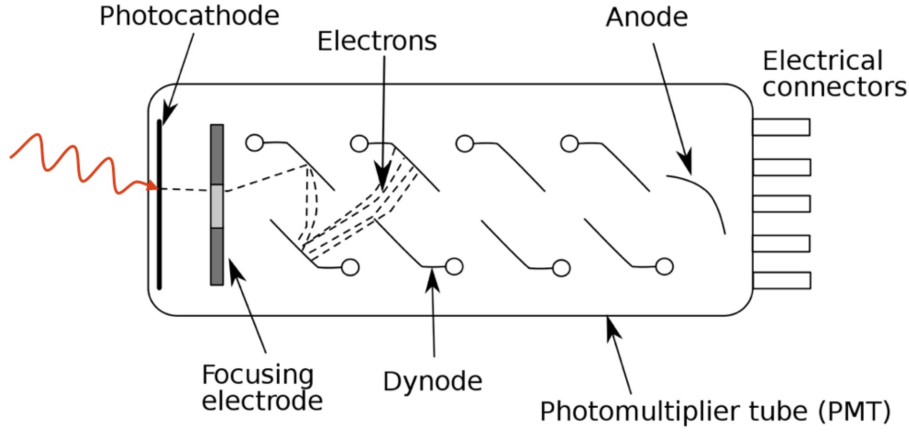


Figure 1: Photomultiplier tube (PMT) used to transform a single photon into a measurable electric signal [5]

- Discriminator: gives a square *out* signal of adjustable width if an *in* signal above a certain adjustable threshold is received.
- Delay module: delays the received signal by an adjustable time.
- Coincidence units *and* ( $\wedge$ ) and *or* ( $\vee$ ): perform the *and* or *or* logic operations on the received signals and give the result as the *out* signal.
- Gate: gives a positive signal for an adjustable duration.

### 3.2 Magnetic field

A Helmholtz coil generates a magnetic field

$$B_1(x) = \frac{\mu_0 n I R^2}{2(R^2 + x^2)^{3/2}} \quad (18)$$

where  $n$  is the number of spires,  $I$  is the current through the spires and  $R$  is the radius of the coils. This means that in the middle of the two coils at  $x = d/2$  the total magnetic field will be given by

$$B = 2B_1(d/2) = \frac{\mu_0 n I R^2}{(R^2 + (d/2)^2)^{3/2}} \quad (19)$$

Here the number of spires is  $n = 598$ , the current passing through the spires is  $I = (4.01 \pm 0.01)$  A, the radius of the coils  $R = (0.49 \pm 0.01)$  m and the distance between the two coils is  $d = (0.58 \pm 0.02)$  m. Thus,  $B = (3.92 \pm 0.13)$  mT. This value was verified using a Gauss meter and gave an almost uniform magnetic field between the coils of  $(6.3 \pm 0.3)$  mT.

## 4 Experimental setup

The detector setup consists of 4 scintillator plates placed horizontally, two above and two below a copper plate of  $(1.0 \pm 0.1)$  cm thickness as shown by Figure 2. The copper plate's purpose

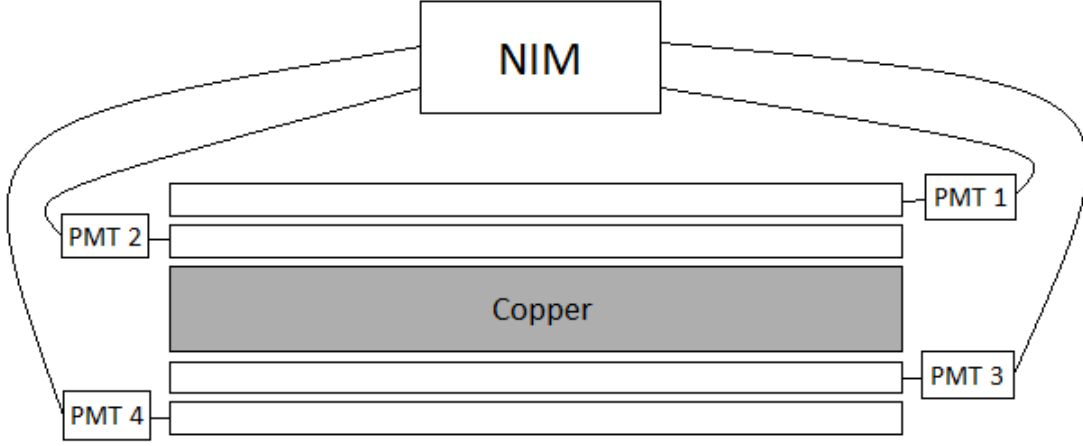


Figure 2: Experimental setup: particle detection apparatus composed of a copper plate between four scintillators connected to four PMTs; the lifetime measurement uses NIM connect to the PMTs to set up a trigger scheme

is to stop the cosmic muons so that they will decay between the scintillators. This stopping process is mainly done through ionisation and thus, the energy loss of the particles is described by the Bethe-Bloch function. A trigger scheme can then be set up using NIM, which will permit only the collection of data concerning the decay of a cosmic muon inside the apparatus.

#### 4.1 Trigger scheme

To measure the time taken for the muon to decay inside the apparatus, a timer has to be started and stopped when appropriate conditions are met. The condition for a start signal is that the two top scintillators are triggered but not the bottom two (call this signal  $top \equiv 1 \wedge 2 \wedge \bar{3} \wedge \bar{4}$ ). This is done so that the timer starts when a particle coming from above is detected, which is more likely for cosmic muons, but does not go straight through the apparatus and trigger the bottom scintillators. This means that the muon is stopped in the copper plate. A delay signal of 51 ns is then imposed on the start signal so that the latter cannot also trigger the stop signal. The latter occurs when a gate, triggered by the delayed start signal, is open and when a  $top \vee bottom$  signal (where  $bottom \equiv \bar{1} \wedge \bar{2} \wedge 3 \wedge 4$ ) is detected. The purpose of the gate is to give a window of time during which the muon can decay and its lifetime can be measured after which, the measurement is cancelled and the timer is started again at the next start signal.

#### 4.2 PMT voltage calibration

Not all the PMTs have a completely equal response, this means that they must be calibrated in such way that all of them have the “same” response. To this aim, we recorded the number of counts,  $N$ , for each PMT at constant discriminator-unit-threshold,  $T$ , through a range of different operating voltage values,  $V$ . With the resulting data, one can extract the values of  $V$  at which all PMTs have a chosen response of  $\ln N = 8.5$ . The data and fitting lines are shown in Figure 4 and obtained values for  $V$ , in Table 1.

## 4 EXPERIMENTAL SETUP

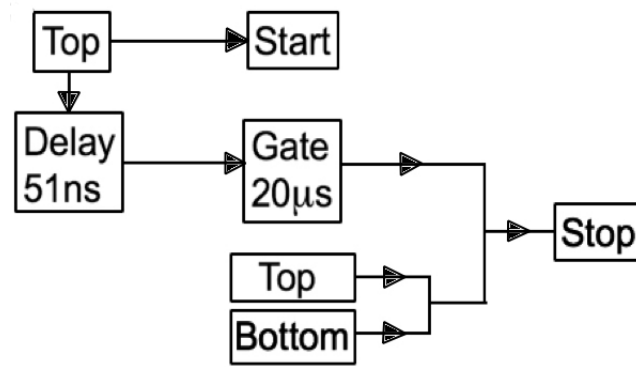


Figure 3: Trigger scheme used to start a stopwatch at the arrival of a cosmic muon and stop it when its decay products exit the apparatus

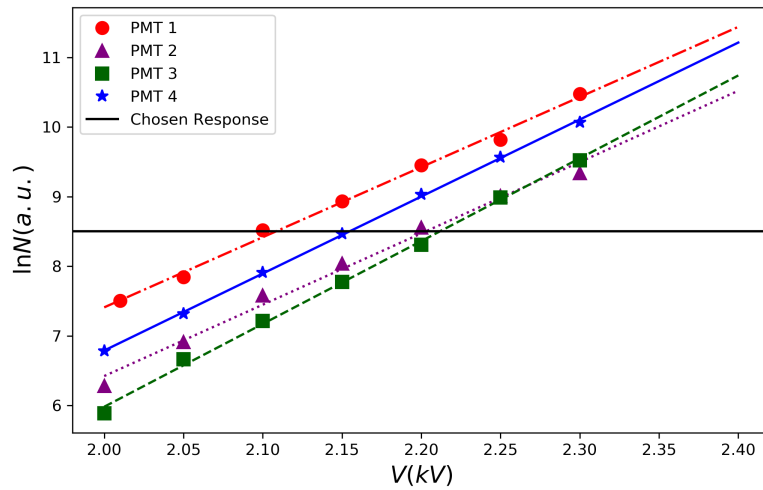


Figure 4: Data and fitting curves for the PMT calibration process. The horizontal line shows the response value chosen.

PMT #	V (kV)
1	2.11
2	2.20
3	2.21
4	2.15

Table 1: Operating voltages of each PMT for a 4.5V threshold

### 4.3 Discriminator threshold calibration

In order to be able to discriminate the signal of the muon decay from the background, it is necessary to adjust the discriminator threshold in such a way that the latter is as low as possible. For this, the counts obtained from each PMT were measured during a 10s lapse, for different values of the threshold  $T \in [0.9, 10.25]\text{V}$ . These measurements were taken in the presence of a  $^{60}\text{Co}$  sample, a  $^{137}\text{Cs}$  one and no sample.



## 4 EXPERIMENTAL SETUP

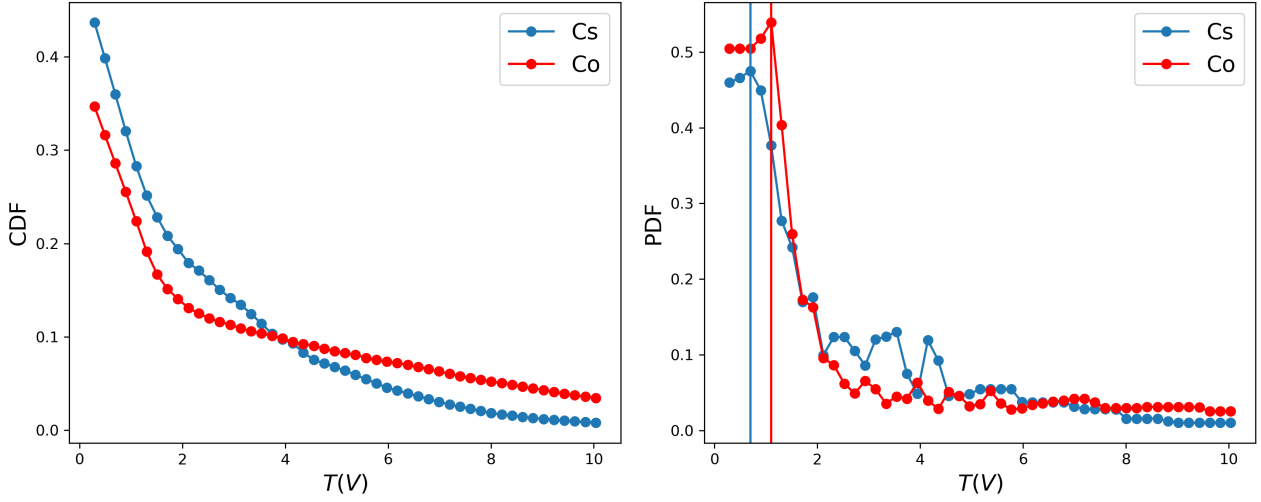


Figure 5: Left: Threshold calibration measurements correspond to a Cumulative Density Function (CDF). Right: The Probability Density Functions (PDF) associated.

The plastic scintillator used in the experiment favors the detection of the Compton-scattered electrons over the photopeak. This means that one has to concentrate on the Compton plateau and, more precisely, on the Compton edge. A rather short computation shows us that this edge is given by

$$E_e^{max} = \frac{2E_\gamma^2}{m_e + 2E_\gamma}, \quad (20)$$

where  $m_e$  is the rest mass of the electron and  $E_\gamma$  is the energy of the photon emitted in the decay. The values  $E_e^{max,Co} = 0.96$  MeV and  $E_e^{max,Cs} = 0.48$  MeV were obtained. The results of these measurements are shown in figure 5. The vertical lines are the selected values of  $T$  for the Compton edge, these are to be compared with the computed  $E_e^{max}$  to map from  $E$  to  $T$  and choose the energy values we would like our experiment to ignore.

In a three body disintegration, the minimum energy of a decay particle is its mass energy, when it is at rest in the center of mass reference frame. Since the electron (positron) is the particle which will be detected, it is the one concerned in these considerations. It's minimum energy is  $E_e^{min} = 0.511$  MeV. On the other hand, the maximum energy of a decay particle, taking again the electron (positron), is given by:

$$E_e^{max} = \frac{m_\mu^2 + m_e^2}{2m_\mu} \quad (21)$$

Therefore, since  $m_\mu = 105.66$  MeV [1],  $E_e^{max} = 52.8$  MeV. Furthermore, energy spectra of electrons from muon decay show a peak at about 50MeV[6]. Therefore, an energy threshold of  $E = 5$  MeV is chosen as this value allows the majority of electrons (positrons) to be detected while avoiding most of the background produced by Compton effect seen in figure 5. With the values obtained from the spectra (PDF) reconstruction, a desired threshold of  $T = 4.53$  V was obtained. It should be clarified that the voltage values for  $T$  have no actual physical significance and are obtained by measuring the voltage on the threshold of the discriminator units with a voltmeter.

## 5 Results

### 5.1 Muon lifetime

The data obtained shows the number of muon decays against their decay time. Since this distribution is in fact the one given by equation (5), the average lifetime of the muon can be found by fitting this equation to the data, leaving  $\tau$  and  $N_0$  as a fit parameters. However, since the positive and negative muons present with different lifetimes in matter, the data can be fitted to a double exponential (equation (22)) to obtain both these lifetimes.

$$N(t) = N_{0+}e^{-\frac{t}{\tau^+}} + N_{0-}e^{-\frac{t}{\tau^-}} + b \quad (22)$$

Here,  $b$  accounts for constant background noise,  $\tau^+ = \tau_d$  is the decay lifetime of positive muons and  $\tau^- = \tau_c$  is the decay lifetime of negative muons which undergo nucleon capture. Furthermore, since the capture lifetime  $\tau_c$  is smaller than the decay lifetime  $\tau_d$ , the contribution of the former on the exponential will be important for small  $t$  and negligible for larger  $t$ . Therefore, to obtain a better value of  $\tau_d$ , an exponential fit can be done only to the tail of the data.

The first set of data obtained, shown by the initial data curve in Figure 6, did not present the expected exponential distribution, or linear distribution on a semi-logarithmic scale.

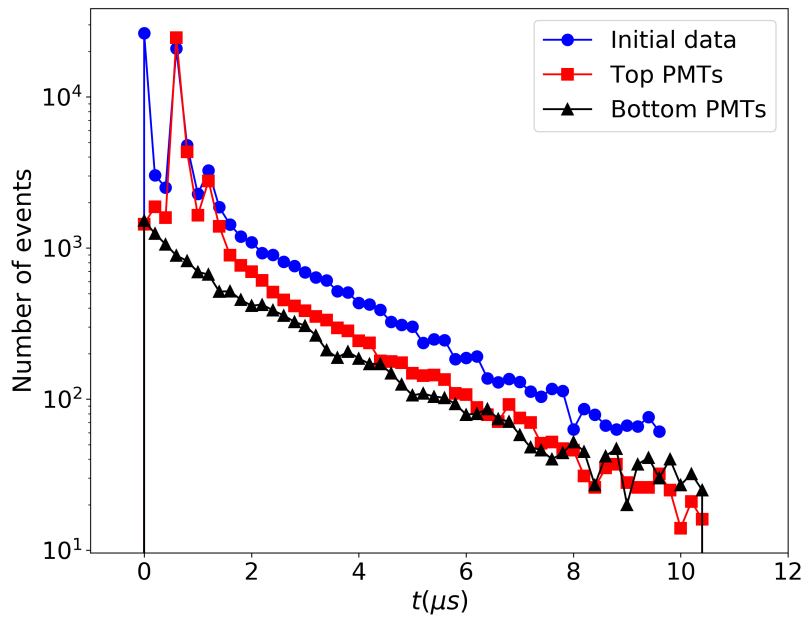


Figure 6: Semi-logarithmic plot of the number of events against decay time for the initial measurements: top and bottom PMTs, only top and only bottom PMTs.

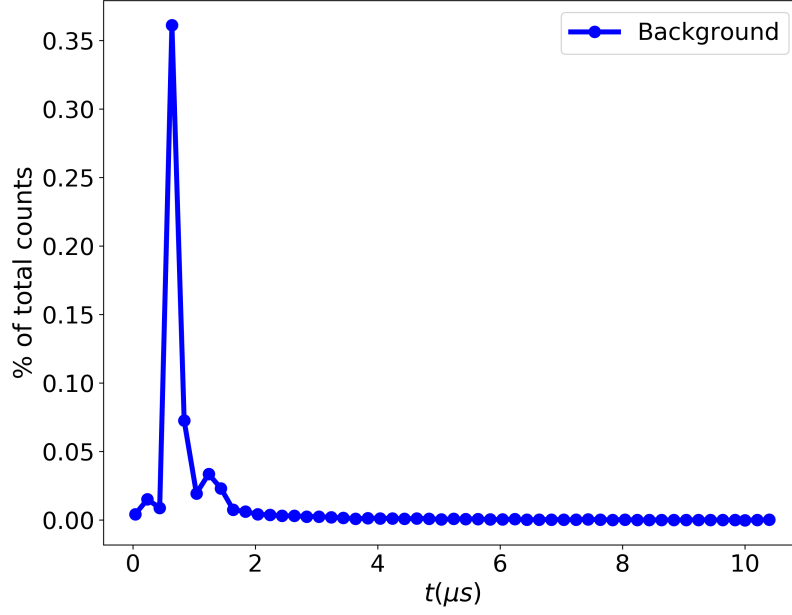


Figure 7: Background noise estimated from the subtraction of the bottom data from the top data

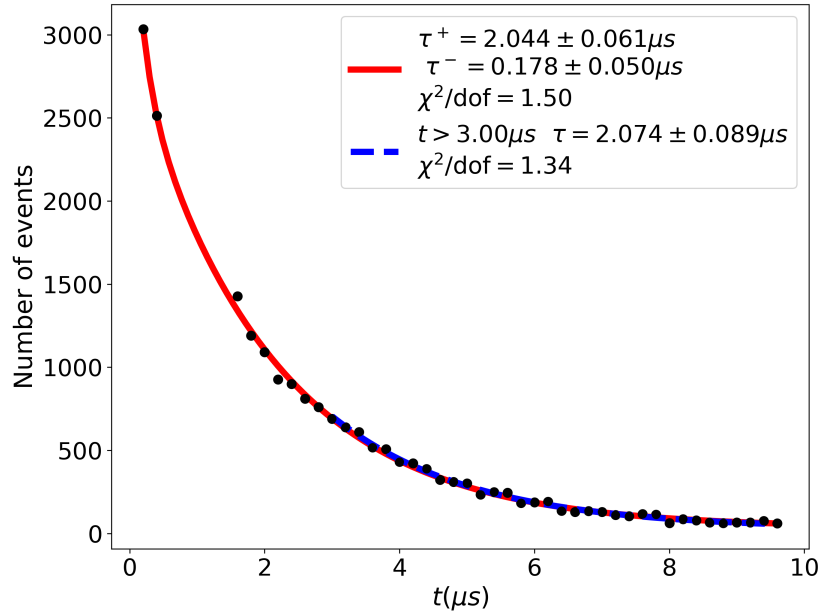


Figure 8: Fit to top and bottom joint data after removing data points affected by the background shown in figure 7. Red (continuous) curve shows the double-exponential fit while the Blue (dashed) curve shows the single exponential fit to the tail.

Indeed there are several peaks of very large amplitude which modify the distribution, rendering it impossible to fit. The stop signal was then separated into top and bottom stop signals,

giving two sets of data corresponding to decay products exiting through the top or bottom of the apparatus. This showed that the data obtained through the top two PMTs is dominated by background noise, whereas the bottom two PMTs give the expected exponential distribution (Figure 6). By subtracting the bottom data from the top data, one can obtain the background noise shown in Figure 7. Because of the statistical nature of the data, it cannot be normalized to subtract the background noise from the original combined data to obtain a reliable dataset. It is concluded that the best approach is to completely eliminate the data points corresponding to the highest 5 local maxima of the noise. An exponential fit can therefore be applied, giving the result of Figure 8.

Since the data obtained using both top and bottom PMTs to trigger the stopping of the clock implies having to remove data, further results are obtained taking only data acquired when the stop signal comes from the two bottom PMTs. This way, only constant background noise has to be considered and data points do not need to be removed. When allowing the data acquisition to run for two weeks without a magnetic field applied, the resulting distribution is shown on Figure 9.

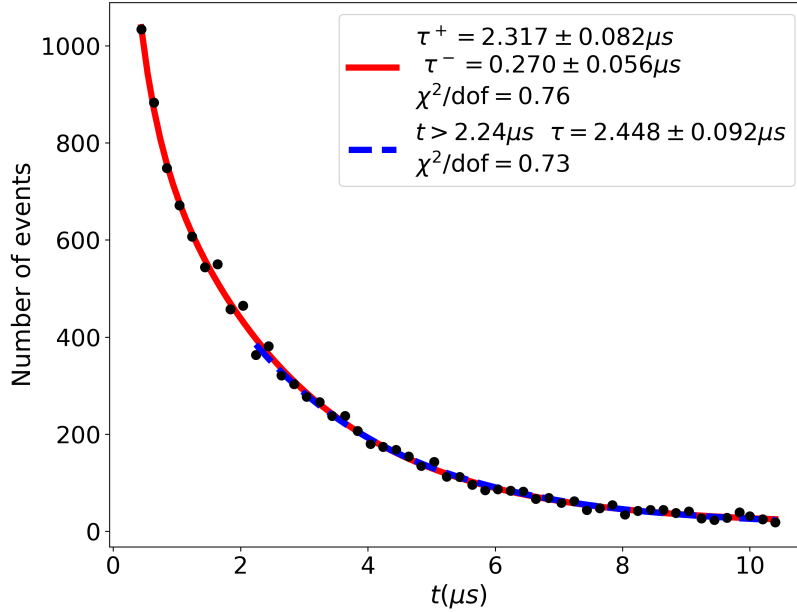


Figure 9: Data acquisition over two weeks: exponential fits of negative and positive muon decay contributions over the whole time scale (red continuous line) as well as the exponential fit of tail data (blue dashed line).

The double exponential fit thus gives a muon decay lifetime of  $\tau^+ = \tau_{\mu,d} = 2.317 \pm 0.082 \mu s$  and a capture lifetime of negative muons  $\tau^- = \tau_{\mu,c} = 0.270 \pm 0.056 \mu s$ . The goodness-of-fit measure was computed and gave  $\chi^2/DOF = 0.76$ . Figure 9 also allows to notice that the fit done only to the tail of the data ( $t > 2.24 \mu s$ ) results in a decay lifetime of  $\tau_{\mu,d} = 2.448 \pm 0.092 \mu s$  with a goodness-of-fit  $\chi^2/DOF = 0.73$ . The two values of the decay lifetime  $\tau_{\mu,d}$  are within each other's uncertainty ranges.

## 5.2 $g$ -factor measurement

When a magnetic field is applied, the precession of the muons around the field direction translates into a modulation of the recorded signal following equation (17). Data collected for a period of two weeks during which a magnetic field of magnitude  $B = 6.3 \pm 0.3 \text{ mT}$  was applied to the apparatus was fitted to this function. In order to do this, the decay lifetime was fixed to  $\tau = 1.958 \mu\text{s}$  which was obtained by performing a single exponential fit to the data taken in absence of magnetic field (see Appendix A). The result is shown in Figure 10.

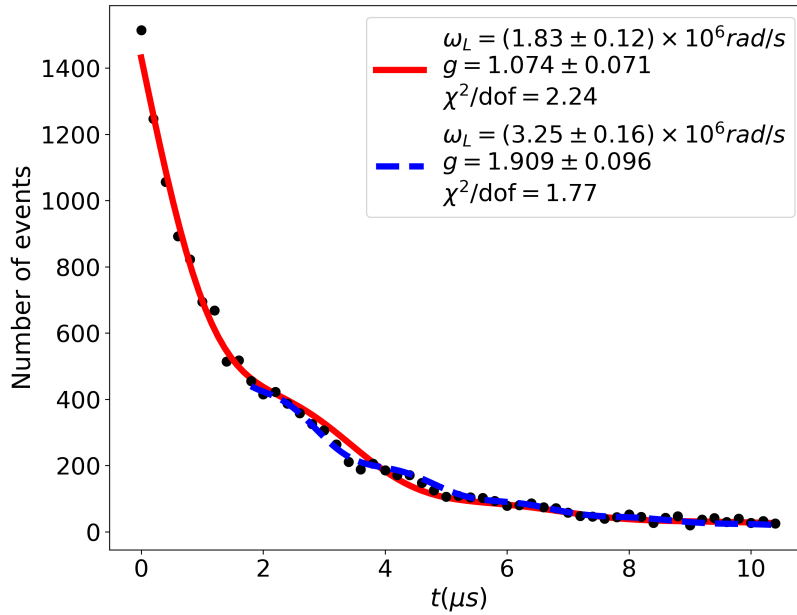


Figure 10: Modulated exponential fit of data obtained when applying a magnetic field  $B = 6.3 \pm 0.3 \text{ mT}$  in the apparatus. Red (continuous) curve is a single-exponential fit to all the data while the blue (dashed) curve is the fit to the tail  $t > 2.24 \mu\text{s}$

The  $g$ -factor value can be deduced from the Larmor frequency obtained from the fit. Thus  $g = 1.074 \pm 0.071$ . Furthermore, the fit has  $\chi^2/DOF = 2.24$ .

Following the fact that the negative muon's contribution to the data falls off much faster than the positive muon's, and since we are only fitting one exponential to the modulated signal, the fit is restricted to the tail ( $t > 2.24 \mu\text{s}$ ) of the measured distribution. In this case, the restricted value of  $\tau$  must also be used. Thus, the lifetime is fixed to  $\tau = 2.448 \mu\text{s}$  obtained for a single-exponential fit to the data when no magnetic field was applied (see Appendix A). The resulting fitted data is shown by Figure 10, where the value of the Larmor frequency is  $\omega_L = (3.250 \pm 0.161) \times 10^6 \text{ rad s}^{-1}$ . This translates to a  $g$ -factor of  $g = 1.909 \pm 0.096$ . This value is closer to the expected value  $g = 2$ . Furthermore, the goodness-of-fit is  $\chi^2/DOF = 1.77$ , which is closer to 1 than that obtained for the fit of the entire data of Figure 10, indicating a better correlation between data and fit.

## 6 Discussion

In order to account for all decay products leaving the apparatus after a muon stopped and decayed inside the copper plate, both the bottom and top PMTs were allowed to stop the clock. However, the data initially obtained this way showed an unexpected behaviour credited to background noise, as shown by Figure 6. The peak at  $t \approx 0 \mu\text{s}$  is most likely due to an undesired overlap between the *top* and *bottom* signals caused by their different widths. Since these two signals no longer interact with each other when recorded individually, such peak is not present in the data obtained from the top and bottom PMTs separately (the triangle and the square-marked curves respectively) of Figure 6.

In order to remove this noise, several points were removed from the data to obtain the expected exponential distribution (Figure 8). However, the measurement of the g-factor required to separate the top and bottom stop signals and therefore separate the data into counts obtained when the decay products exited through the top (top data) or the bottom (bottom data) of the apparatus. In doing so, it was noticed that the data obtained when the top PMTs stopped the clock presented with the same background noise as the initial data but the bottom data showed the expected exponential distribution. The experiment without magnetic field was thus repeated, separating top and bottom data. Their subtraction allowed to isolate the background noise as shown by Figure 7. This in turn enabled to take away the data points affected by noise in the initial data and gave the results of Figure 8.

Removing data points to account for background noise implies reducing the number of counts used in the fit. To obtain a better statistic, only the bottom data was used, where only constant background noise needs to be accounted for. Furthermore, using only bottom data also brings the goodness-of-fit value  $\chi^2/DOF$  closer to 1. The results are presented in Figure 9. The decay lifetime obtained is  $\tau_{\mu,d} = 2.317 \pm 0.082 \mu\text{s}$  through the double exponential fit, and  $\tau_{\mu,d} = 2.448 \pm 0.092 \mu\text{s}$  through the fit of the tail. These values are coherent when considering their uncertainties, that is, they fall within each other's uncertainty range. However, the tabulated value of the muon lifetime  $\tau = (2.196\,981 \pm 0.000\,002) \mu\text{s}$  [1] is not within either's margin of error. However,  $\frac{|2.317-2.197|}{0.092} = 1.304$ , which means that the difference between the experimental and the tabulated value is only 1.304 times the error. Furthermore, it should be noted that only statistical errors have been considered and not the systematic errors of the apparatus. Therefore, if we consider that these are of the order of the statistical errors, then the tabulated value would indeed be within the margin of error.

On the other hand, the experimental lifetime of the negative muon in copper, that is  $\tau_c$  is given by Figure 9 which shows an experimental value of  $\tau_{\mu,c} = (0.270 \pm 0.056) \mu\text{s}$ . The value of  $\tau_{\mu,c}$  from literature is not within the the experimental result's margin of error. However, if this value is obtained from the initial data where the background noise is removed, then  $\tau_{\mu,c} = (0.178 \pm 0.050) \mu\text{s}$ . Here, the value from literature does fall within the margin of error. This indicates, similarly to the case of  $\tau_{\mu,d}$  that not all errors have been considered and that systematic errors need to be taken into account.

When a magnetic field of  $B = 6.3 \pm 0.3 \text{ mT}$  is applied to the apparatus, the precession of the muon's spin around the direction of the field modulates the decay lifetime distribution, allowing to extract the g-factor. This is done through the Larmor frequency (15) which is

## 7 CONCLUSION

left as a fit parameter of the function (17) applied to the data. Figure 10 shows that the value of the g-factor obtained is  $g = 1.074 \pm 0.071$  when fitting the entirety of the data, and  $g = 1.909 \pm 0.096$  when fitting only the tail. The g-factor of muons predicted by the Dirac theory,  $g = 2$  is within the uncertainty margin of the value obtained when fitting the tail of the data. This fit was done fixing the decay lifetime to the value obtained when fitting the tail of the data without applying a magnetic field,  $\tau = 2.448 \mu\text{s}$ . Additionally, the goodness-of-fit in this case is  $\chi^2/DOF = 1.77$  which is closer to 1 than when fitting the entire data, which gives  $\chi^2/DOF = 2.24$ . In the latter case, the g-factor obtained is further from the theoretical value. This could thus be attributed to a bad fit.

## 7 Conclusion

The first part of the experiment consisted in acquiring a deeper understanding of the experimental setup, during which the PMT working voltages were calibrated so as to have similar responses. Additionally, the discriminator unit thresholds were calibrated in order to avoid the recording of background events as much as possible. Nevertheless, a significant amount of unaccounted-for background was recorded by the top PMTs (1 and 2) as shown by Figure 6. A further analysis on the background sources or calibration procedure might give some clues on the source of such a high peak at  $t \approx 1 \mu\text{s}$ .

To correct this noise, a pure background signal (Figure 7) is extracted. However, the statistical nature of the data makes it difficult to correctly normalize the background in order to subtract it from the noisy data. The data obtained with the stop signal coming from the bottom PMTs was therefore used as it did not present with the same dominating background.

Using this, the two quantities this experiment intended to measure, the muon lifetime and g-factor, were found. Firstly, the average decay lifetime of muons was measured to be  $\tau_{\mu,d} = (2.317 \pm 0.082) \mu\text{s}$ , with a deviation of 5% from the value found in literature  $\tau_d = 2.196981 \pm 0.000002 \mu\text{s}$  [1]. For the negative muons, the capture lifetime in copper obtained is  $\tau_{\mu,c} = (0.270 \pm 0.056) \mu\text{s}$  which has a 69% deviation from the tabulated value  $\tau_c = 0.16 \mu\text{s}$  [3]. Even though the tabulated values are not within the uncertainties, it is important to bear in mind that the analysis only takes into account the statistical error in the estimation of the fit parameters and that systematic errors are not included.

Secondly, the value of the g-factor was found to be  $g = 1.909 \pm 0.096$  which includes the value  $g = 2$  predicted by Dirac theory in its margin of error. However, the important uncertainty of this experimental value means that the anomalous magnetic moment cannot be found. In order to do this, more accurate measurements would need to be done, for example by taking more data, varying the magnetic field and using more accurate apparatus.

## References

- [1] Patrignani C. et al. (Particle Data Group), *Particle Physics Booklet*, Chin. Phys. C, 40, 100001 (2016)
- [2] Nagamine, K., *Introductory Muon Science*, Cambridge: Cambridge University Press. (2003)
- [3] Suzuki', T., Measday, D. F., Roalsvig, J. P. (1987). *Total nuclear capture rates for negative muons* (Vol. 35). Retrieved from <https://journals.aps.org/prc/pdf/10.1103/PhysRevC.35.2212>
- [4] Walter, M., Gerlich, C., *Measurement of Muon Properties in the Advanced Students Laboratory*, Heidelberg University (2002)
- [5] Tadday, K. A., *Scintillation Light Detection and Application of Silicon Photomultipliers in Imaging Calorimetry and Positron Emission Tomography*, Ruprecht-Karls University Heidelberg, (2011).
- [6] Barlow, J. et. al., *The momentum spectrum of electrons from muon decay*, Proc. Phys. Soc. 84 239 (1964)
- [7] Lebigot, E. O. (n.d.). Uncertainties: a Python package for calculations with uncertainties. Retrieved from <https://pythonhosted.org/uncertainties/>



## Appendix

### Appendix A

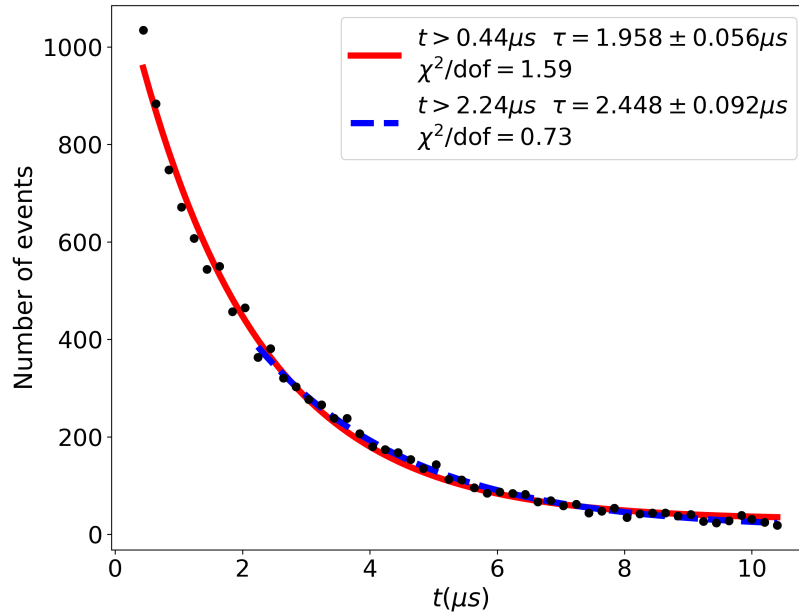


Figure 11: Single exponential fit of data acquired during two weeks in order to obtain a value of  $\tau$  to fix in the fit when applying a magnetic field